

Joule heating effect on radiating MHD slip flow and heat transfer over an exponentially stretching permeable sheet embedded in porous medium with heat source

Rajendra Kumar Meena¹*, Deepak Kumar¹, and Ravindra Kumar¹

¹Department of Mathematics, Vivekananda Global University, Jaipur (Raj.), India

Abstract. This article inquires into the steady Joule Heating Effect on Radiating Thermal transfer and MHD slip movement across an exponentially extending permeable sheet embedded within a medium that is porous with a source of heat. Using similarity transformations, the border layer problem is formulated and transformed into a nonlinear ordinary differential equation. The Runge-Kutta fourth order approach is then used to find the numerical result using the shooting methodology. Joule heating is widely applied in domestic and industrial devices to convert electrical energy into heat, primarily using high-resistance materials like Nichrome. Major applications include heating appliances (iron, toaster, kettle, oven), safety devices (fuses), and lighting (incandescent bulbs). The impact of different physical characteristics on temperature and velocity distributions is conferred quantitatively and illustrated graphically. Heat and the flow rate rise as the Prandtl number rises Pr , mixed convection restriction λ , Suction restriction S , and exponential restriction N , while reverse effect is seen in magnetic restriction M , radiation restriction Ra , thermal slip restriction S_t , and heat Source restriction δ . Skin friction coefficient and Nusselt number both are increasing function of radiation restriction Ra , while reverse effect is seen in magnetic restriction M , and exponential restriction N . Skin friction coefficient is increasing function and Nusselt number is decreasing function of restriction velocity slip restriction S_v , while reverse effect is seen in radiation restriction Ra , and heat Source restriction δ .

Introduction: The study of heat transmission over expanding porous sheets in hydromagnetic electrically conducting fluid flow is crucial for many modern metalworking and metallurgical operations. Numerous scholars are interested in this topic due to its potential uses in nuclear power reactors, soil sciences, astrophysics, geophysics, etc. Electromagnetic forces are used to pump liquid sodium around during the cooling phase of nuclear fission reactors. MHD equations as well as finite element evaluation a sophisticated method used in medical science to accurately distribute medication to cancer-affected tissues, are utilized to investigate how the bloods magnetic fluid particles interact with the surrounding magnetic field. In the process of filtering particles from liquids and extracting crude oil from rock pores, fluid flow across porous media is now a predictable subject to investigate. Applications of fluid movement via porous medium in the environment include the movement of groundwater through rocks and soil, which is crucial for pollution prevention and agriculture. The suction/injection process is crucial for numerous engineering tasks, including radial diffuser design, thrust bearing design, and thermal oil recovery. In chemical reactions, suction is sometimes used to eliminate reactants. Natural heat sources and sinks, such as air, ground, water, etc., are used in heat pumping technology. Compressors, freezers, and air

conditioners all use this technology. [Char 1], investigated heat transport in the laminar boundary layer on a continuous, linearly stretched surface to which suction or blowing is applied. The viscous incompressible flow across a stretching sheet was studied by [Kumaran and Ramanaiah 2]. [Magyari and Keller 3], studied the similarity solutions characterizing the steady plane boundary layers on an exponentially stretched continuous surface with an exponential temperature distribution. [Elbashbeshy 4], considered similarly solutions of the laminar equations for the boundary layer that describe flow and heat in a quiescent fluid driven by an stretchable surfaces that are under suction are investigated numerically. [Andersson 5], studied slip flow past a stretching surface. The analysis of viscous flow caused by a shrinking sheet was done by [Miklavcic and Wang 6]. [Aman and Ishak 7], introduced the topic of mixed convection boundary layer flow next to a extending a sheet vertically in an incompressible electrically conducting fluid when a transverse magnetic field is present. [Pal and Hiremath 8], examined the heat transfer properties in the laminar boundary layer flow of an incompressible viscous fluid over an unstable stretched sheet situated in a porous medium when viscous dissipation and internal absorption or generation are present. [Salleh et al., 9], investigated the steady boundary layer flow and heat transfer across a stretching sheet with Newtonian

* Corresponding author: rajendrameena0135@gmail.com

heating, where the heat transfer from the surface is proportional to the local surface temperature. [Ishak 10], investigated how radiation affected the MHD boundary layer flow of a viscous fluid across an exponentially extending sheet. Heat transmission on a generalized stretching/shrinking wall with a convective boundary condition was investigated by [Yao et al., 11]. [Cortell 12], examined the flow and heat transfer of a viscous incompressible fluid in a porous media across a permeable stretched surface while accounting for thermal radiation and the temperature-dependent fluctuation of thermal conductivity. The three-dimensional flow of a Jeffery fluid across a sheet that is stretching linearly was examined by [Hayat 13]. [Soid et al., 14], examined MHD boundary layer flow in a viscous fluid over a stretching sheet with radiation effects, assuming that the temperature and stretching velocity of the sheet obey a power law. [Mandal and Mukhopadhyay 15], presented the heat transfer and boundary layer flow towards an exponentially expanding porous sheet buried in a porous medium with a fluctuating surface heat flux. [Mukhopadhyay 16], investigated the heat transfer and boundary layer flow towards a porous exponential stretching sheet in the presence of a magnetic field. In place of no-slip conditions at the interface, velocity slip and thermal slip are taken into account. The temperature equation includes a factor for thermal radiation. [Sarif et al., 17], studied steady boundary layer flow and heat transfer across a stretching sheet with Newtonian heating, where the local surface temperature determines how much heat is transferred from the surface. [Singh and Makinde 18], presented the mixed convection flow with slip and convective heat transfer along a vertical plate that moves continuously while a uniform free stream is present. Both the plate's velocity and the free stream's velocity are traveling in the same way.

Mathematical formulations. An electrically conducting, viscous, incompressible fluid flows steadily in two dimensions in a laminar flow through a flat, exponentially non-conducting extending porous sheet embedded in a porous medium with non-uniform permeability. We take the x -axis along the stretched sheet and the y -axis perpendicular to it. The fluid can only flow if $y > 0$. The flow, which stretches the wall while keeping the origin immobile, is produced by two equal and opposing forces operating along the x -axis. It is supposed that the surface is extremely elastic and that it is stretched with velocity $U = U_0 e^{\frac{Nx}{L}}$ in the x -direction. In the y -direction, a non-uniform magnetic field $B^* = B_0 e^{\frac{Nx}{2L}}$ is applied. The induced magnetic field is disregarded because it is presumed that the magnetic Reynolds is insignificant. The temperature of sheet T_w is

believed to be changeable and to be given by $T_w = T_\infty + T_0 e^{\frac{Nx}{2L}}$. There is also a non-uniform heat source used.

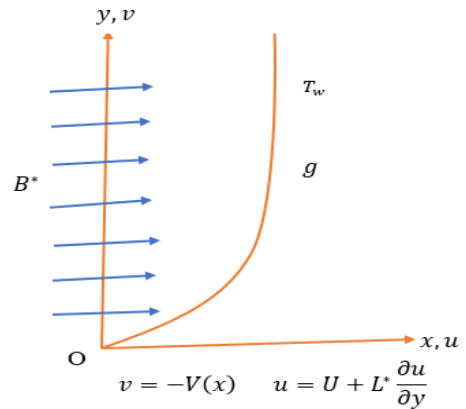


Fig. 1. Sketch of the physical problem.

The principal equations of continuity, momentum, and energy are written as

$$\frac{\partial u}{\partial x} + \frac{\partial v}{\partial y} = 0, \tag{1}$$

$$u \frac{\partial u}{\partial x} + v \frac{\partial u}{\partial y} = v \frac{\partial^2 u}{\partial y^2} - \left(\frac{\sigma B^{*2}}{\rho} + \frac{v}{K^*} \right) u + g \beta_T (T - T_\infty), \tag{2}$$

$$u \frac{\partial T}{\partial x} + v \frac{\partial T}{\partial y} = \frac{k}{\rho c_p} \frac{\partial^2 T}{\partial y^2} + \frac{Q^*}{\rho c_p} (T - T_\infty) + \frac{\mu}{\rho c_p} \left(\frac{\partial u}{\partial y} \right)^2 + \frac{\sigma B^{*2}}{\rho c_p} u^2 - \frac{1}{\rho c_p} \frac{\partial q_r}{\partial y}, \tag{3}$$

where the velocity components in the x and y directions are denoted by u and v respectively, volumetric coefficient of thermal growth is β_T , $\nu = \left(\frac{\mu}{\rho} \right)$ is the kinematic viscosity, thickness of fluid is L , electrical conductivity is σ , fluid temperature is T , fluid thermal conductivity is k , acceleration is g , $Q^* = Q_0 e^{\frac{-Nx}{L}}$ is the non-uniform heat source, $K^* = K_0 e^{\frac{-Nx}{L}}$ represents the medium's irregular permeability and C_p is the specific warmth at unbroken pressure. The corresponding boundary conditions are given by,

$$y = 0 : u = U + L^* \frac{\partial u}{\partial y}, v = -v(x), T = T_w + D^* \frac{\partial T}{\partial y};$$

$$y \rightarrow \infty : u \rightarrow 0, T \rightarrow T_\infty, \tag{4}$$

Where $v(x) = V_0 e^{\frac{Nx}{2L}}$ the suction velocity at the sheet is, $L^* = L_0 e^{\frac{-Nx}{2L}}$ is the velocity slip factor and $D^* = D_0 e^{\frac{-Nx}{2L}}$ is the thermal slip factor. Introducing the similarity variables as

$$\eta = y \sqrt{\frac{U_0}{2\nu L}} e^{\frac{Nx}{2L}}, \theta(\eta) = \frac{T-T_\infty}{T_w-T_\infty}, \psi = \sqrt{2\nu U_0 L} e^{\frac{Nx}{2L}} f(\eta), u = U_0 e^{\frac{Nx}{L}} f'(\eta), v = -N \sqrt{\frac{\nu U_0}{2L}} e^{\frac{Nx}{2L}} (\eta f'(\eta) + f(\eta)), \quad (5)$$

into equations, Consequently, the equation of continuity is automatically satisfied. The equation of momentum and energy convert into the equation (6) and (7)

$$f''' + Nf f'' - 2Nf'^2 - \left(M + \frac{1}{K}\right) f' + 2\lambda\theta = 0, \quad (6)$$

$$\theta'' = -\frac{Pr}{\left(1 + \frac{4}{3}Ra\right)} \left[Nf\theta' - Nf'\theta + Ec(f'')^2 + MEcf'^2 + 2\delta\theta \right] \quad (7)$$

Where $M = \frac{2\sigma B_0^2 L}{\rho U_0}$ is the Magnetic restriction, $Pr = \frac{\mu C_p}{k}$ is the Prandtl number, $Ec = \frac{U^2}{C_p(T_w-T_\infty)}$ is the Eckert number, $\lambda = \frac{Gr}{Re^2}$ mixed convection restriction where $Gr = g\beta_T(T_w - T_\infty) \frac{L^3}{\nu^2}$ is local Grashof number and $Re = \frac{LU}{\nu}$ is local Reynolds number, $K = \frac{U_0 k_0}{2\nu L}$ is porous medium permeability restriction, $\delta = \frac{Q_0 L}{\rho C_p U_0}$ heat generation/absorption restriction, $Ra = \frac{4\sigma^* T_\infty^3}{kk^*}$ radiation restriction. Now boundary conditions are simplified to

$$\eta = 0, f = \frac{S}{N}, f' = 1 + S_v f'', \theta = 1 + S_T \theta' \eta \rightarrow \infty, f' \rightarrow 0, \theta \rightarrow 0, \quad (8)$$

Where $S = V_0 \sqrt{\frac{2L}{\nu U_0}}$, is suction restriction, $S_v = L_0 \sqrt{\frac{U_0}{2\nu L}}$ velocity slip restriction and $S_T = D_0 \sqrt{\frac{U_0}{2\nu L}}$, is thermal slip restriction.

Coefficient of Skin friction and Nusselt number In terms of the sheet's coefficient of skin friction, the rate of shear stress is determined by

$$C_f = \frac{2\tau_w}{\rho U^2} = \left(\frac{Re_x}{2}\right)^{-\frac{1}{2}} f''(0), \quad (9)$$

Rate of heat transfer at sheet is measured by Nusselt number which is

$$Nu = \frac{1q_w}{k(T_w-T_\infty)} = -(1 + Ra) \left(\frac{Re_x}{2}\right)^{\frac{1}{2}} \theta'(0), \quad (10)$$

Where $\tau_w = \mu \left(\frac{\partial u}{\partial y}\right)_{y=0}$, is walls shear stress and rate of heat transfer $q_w = -k \left(\frac{\partial T}{\partial y}\right)_{y=0} + (q_r)_{y=0}$,

Mathematical process for result

A systematic numerical procedure using a shooting strategy determines the result of Equations (6) through (7)

along with borderline situations (8). The variable quantity is labelled in order to convert the nonlinear equivalences into first order regular differential equivalences i.e.

$$f = f_1, f' = f_2, f'' = f_3, f''' = f'_3, \theta = f_4, \theta' = f_5, \theta'' = f'_5$$

Hence, the system of equations becomes

$$f'_1 = f_2 \quad (11)$$

$$f'_2 = f_3 \quad (12)$$

$$f'_3 = -Nf_1 f_3 + 2Nf_2^2 + \left(M + \frac{1}{K}\right) f_2 - 2\lambda f_4 \quad (13)$$

$$f'_4 = f_5 \quad (14)$$

$$f'_5 = \frac{-Pr}{\left(1 + \frac{4}{3}Ra\right)} \left[Nf_1 f_5 - Nf_2 f_4 + Ec f_3^2 + MEc f_2^2 + 2\delta f_4 \right] \quad (15)$$

The boundary conditions are

$$f_1(0) = \frac{S}{N}, f_2(0) = 1 + S_v f_3(0), f_3(0) = S01, f_4(0) = 1 + S_T f_5(0), f_5(0) = S02, f_2(\infty) = 0, f_4(\infty) = 0 \quad (16)$$

MATLAB software is now utilized to perform calculations and integrate data step-by-step using the Runge-Kutta fourth order method with shooting technique.

Results and discussion

Figs. 2(a) and 2(b) illustrate the belongings of magnetic restriction M on velocity and temperature, correspondingly. The velocity profiles and temperature showed a decrease trend when the magnetic restrictions were increased. This suggests that greater heat flow and lower velocity profiles were the outcomes of higher magnetic restriction values. The Lorentz force is created when water with dielectric characteristics is subjected to an electric field M. The current rate decreases inside the shear layer despite electromagnetisms opposition to flowing processes. A kind of friction coefficient produced by the drag coefficient being affected by the Lorentz force. 3(a) and 3(b) show the effects of changing Prandtl numbers Pr, on velocity and temperature, respectively. The velocity profiles and temperature both showed a increase trend when the Prandtl number were increased. Thus, the observed increase in velocity and temperature outlines with growing Prandtl number is caused by the reduced thermal diffusion and increased temperature gradients, which enhance fluid motion and heat retention. Figs. 4(a) and 4(b) illustrate the effects on velocity and temperature of varying radiation restriction Ra. As the radiation restriction Ra, increases, the temperature and velocity both decreases. Thus, in scenarios where radiation primarily acts as a cooling mechanism,

increasing Ra results in lower temperature and velocity due to increased radiative heat loss and reduced fluid motion. Figs. 5(a) and 5(b) illustrate the effects of varying mixed convection restriction λ , on velocity and temperature, respectively. The velocity profiles and temperature both showed an increase trend when the mixed convection restriction were increased. Thus, as the mixed convection restriction increases, both velocity and temperature outlines show an increasing trend due to stronger buoyancy and enhanced convective heat transfer. Figs. 6(a) and 6(b) show the effects of varying exponential Restriction N , on velocity and temperature, respectively. The velocity profiles and temperature both showed an increase trend when the exponential Restriction is increased. Figs. 7(a) and 7(b) illustrate the effects of varying thermal slip restriction S_t , on velocity and temperature, respectively. The velocity profiles and temperature both showed a decrease trend when the thermal slip restriction is increased. Figs. 8(a) and 8(b) illustrate the effects of varying Suction restriction S , on velocity and temperature, respectively. The velocity profiles and temperature both showed an increase trend when the Suction restriction is increased. Figs. 9(a) and 9(b) illustrate the effects of varying heat Source restriction δ , on velocity and temperature, respectively. The velocity outlines and temperature both showed a decrease trend when the heat Source restriction is increased. Fig. 10 show the effects of varying heat Eckert number Ec on velocity. The velocity outlines showed a decrease trend when the Eckert number is increased. Fig. 11 show the effects of varying heat permeability restriction K on velocity. The velocity outlines showed a increase trend when the permeability restriction is increased. Fig. 12 show the effects of varying heat velocity slip restriction S_v on velocity. The velocity outlines showed a increase trend when the velocity slip restriction is increased.

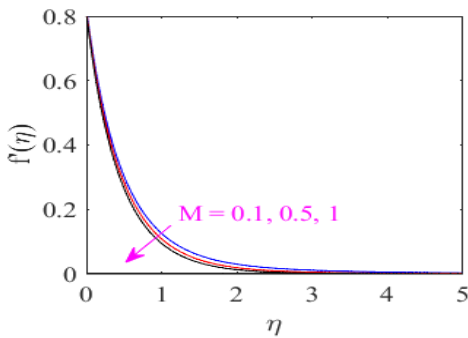


Fig. 2(a). Velocity with η for different Magnetic restriction M .

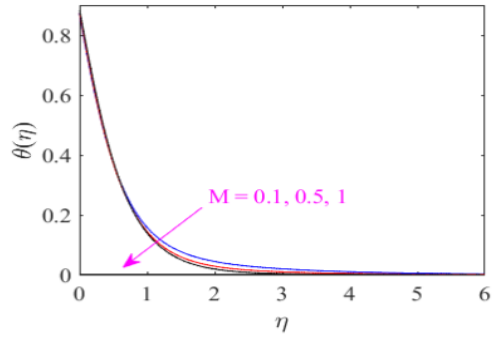


Fig. 2(b). Temperature with η for different Magnetic restriction M .

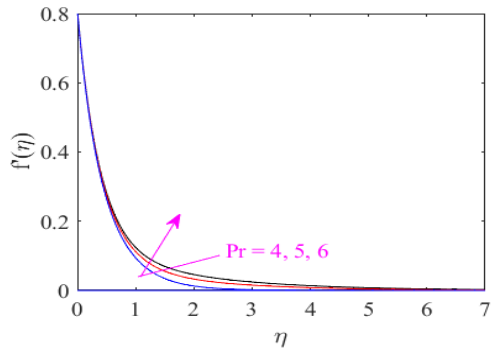


Fig. 3(a). Velocity with η for different Prandtl number Pr .

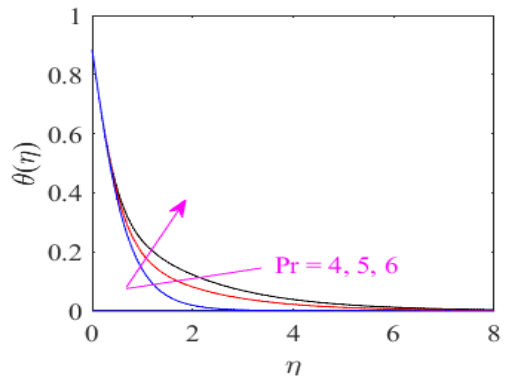


Fig. 3(b). Temperature with η for different Prandtl number Pr .

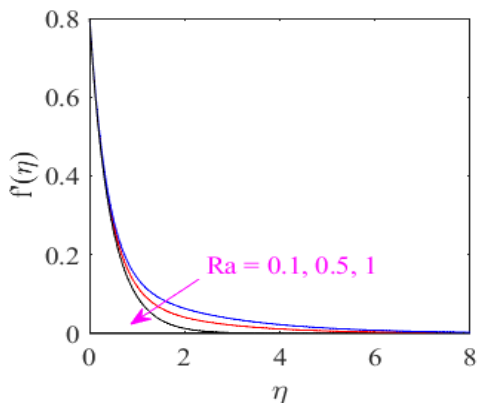


Fig. 4(a). Velocity with η for different radiation restriction Ra .

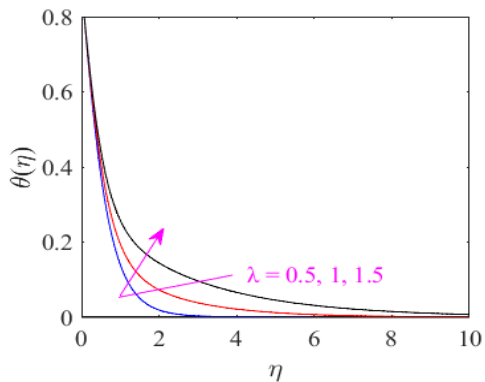


Fig. 5(b). The temperature with η for different mixed convection restriction λ

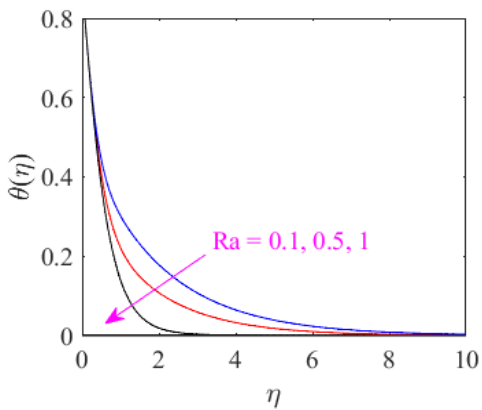


Fig. 4(b). The temperature with η for different radiation restriction Ra .

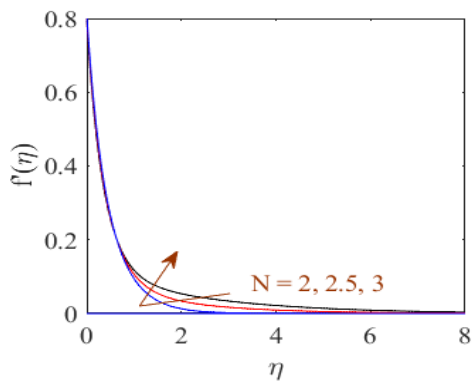


Fig. 6(a). Velocity with η for different exponential Restriction N .

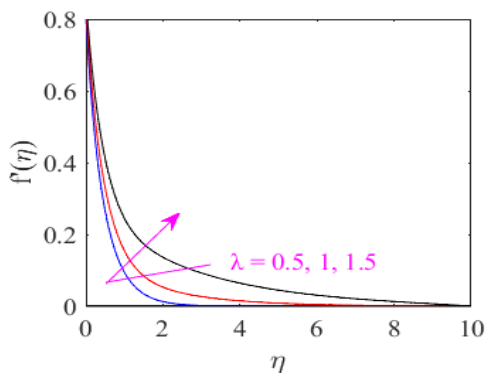


Fig. 5(a). Velocity with η for different mixed convection restriction λ .

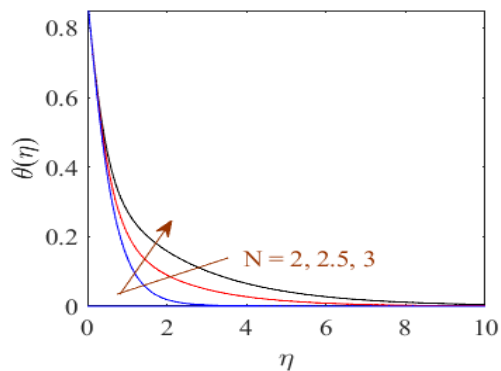


Fig. 6(b). Temperature with η for different exponential Restriction N .

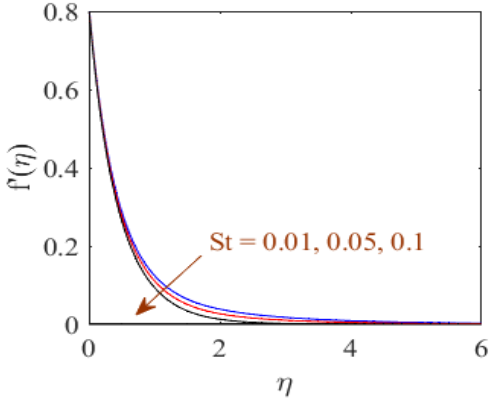


Fig. 7(a). Temperature with η for different thermal slip restriction S_t .

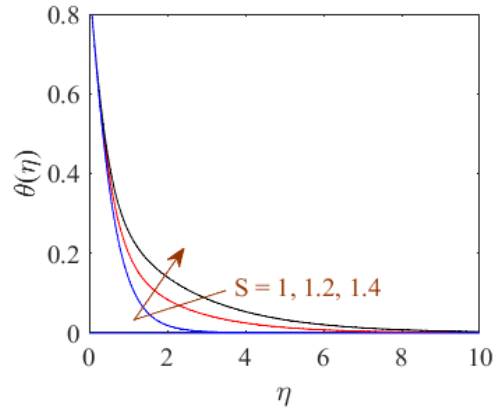


Fig. 8(b). Temperature with η for different Suction restriction S .

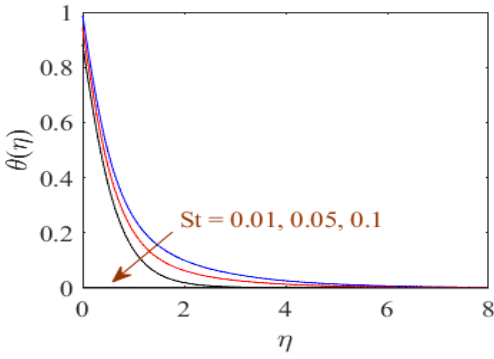


Fig. 7(b). Temperature with η for different thermal slip restriction S_t .

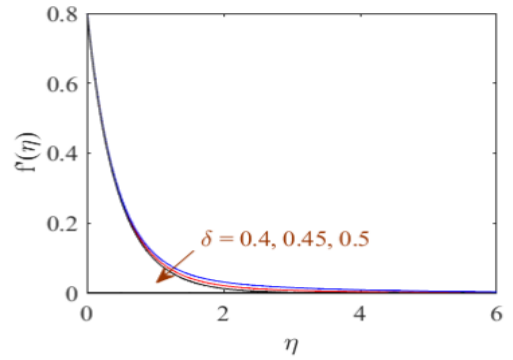


Fig. 9(a). Velocity with η for different heat Source restriction δ .

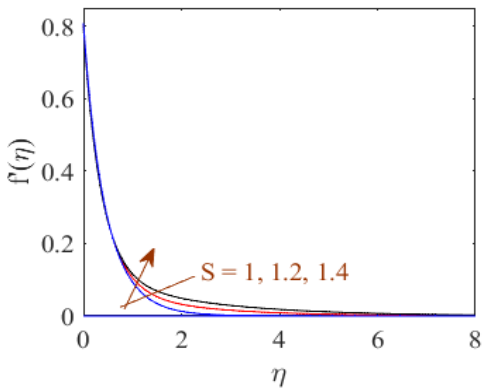


Fig. 8(a). Velocity with η for different Suction restriction S .

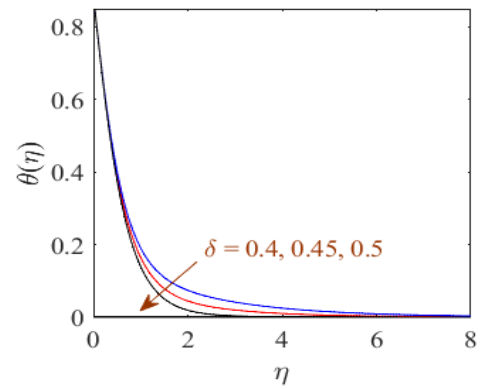


Fig. 9(b). Temperature with η for different heat Source restriction δ .

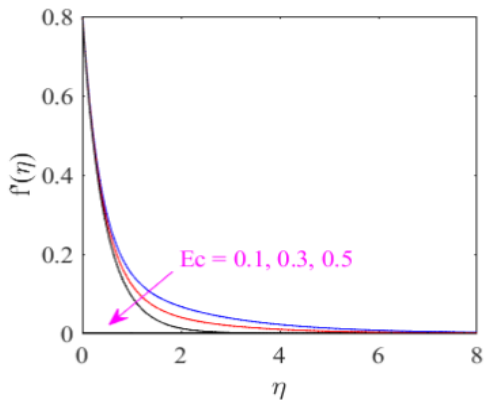


Fig. 10. Velocity with η for different Eckert number Ec .

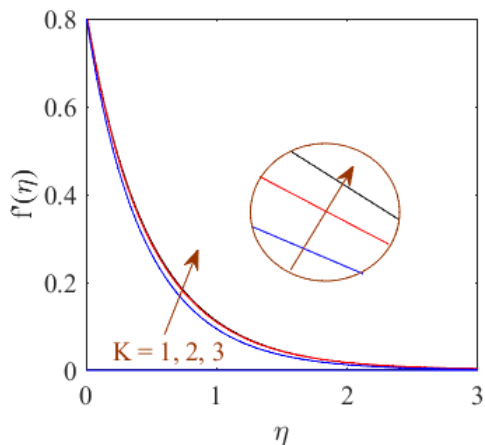


Fig. 11. Temperature with η for different permeability restriction K .

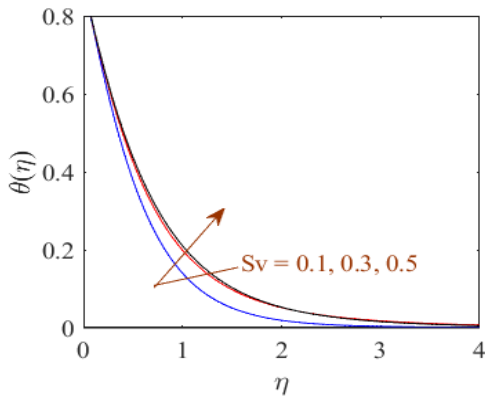


Fig. 12. Temperature with η for different velocity slip restriction S_v .

Table 1 Impact of different non-dimensional controlling factors on skin friction factors $C_f Re_x^{1/2}$ and Nusselt number $Nu_x Re_x^{-1/2}$

Restriction	$C_f Re_x^{1/2}$	$Nu_x Re_x^{-1/2}$
$K = 1$	-1.922535	2.326822
$K = 2$	-1.820000	2.430496
$K = 3$	-1.800000	2.466480
$M = 0.1$	-1.774174	2.560222
$M = 0.5$	-1.845294	2.466762
$M = 1$	-1.922535	2.326822
$N = 2$	-1.922535	2.326822
$N = 2.5$	-1.995535	2.322330
$N = 3$	-2.063751	2.318986
$S_v = 0.1$	-1.922535	2.326822
$S_v = 0.3$	-1.280311	2.326814
$S_v = 0.5$	-0.969903	2.326810
$Ra = 0.1$	-1.879185	1.279752
$Ra = 0.5$	-1.899907	1.745117
$Ra = 1$	-1.922535	2.326822
$\delta = 0.4$	-1.906787	2.326620
$\delta = 0.45$	-1.914960	2.326720
$\delta = 0.5$	-1.922535	2.326822

Table 2 Impact of different non-dimensional controlling factors on skin friction factors $C_f Re_x^{1/2}$

Restriction	$C_f Re_x^{1/2}$
$Pr = 4$	-1.922535
$Pr = 5$	-1.906997
$Pr = 6$	-1.895828
$\lambda = 0.5$	-1.922535
$\lambda = 1$	-1.701409
$\lambda = 1.5$	-1.456336
$Ec = 0.1$	-1.861244
$Ec = 0.3$	-1.890456
$Ec = 0.5$	-1.922535
$S = 1$	-1.922535
$S = 1.2$	-1.970442
$S = 1.4$	-2.019628
$S_t = 0.01$	-1.867633
$S_t = 0.05$	-1.891972
$S_t = 0.1$	-1.922535

Table 3 Impact of different non-dimensional controlling factors on skin friction factors $C_f Re_x^{1/2}$ and Nusselt

number $Nu_x Re_x^{-1/2}$ when $Ra = 0, S_v = 0.1, S_T = 0.1$ and $M = 0$

Restriction	$C_f Re_x^{1/2}$	$Nu_x Re_x^{-1/2}$
$K = 1$	-2.7051005	1.677319
$K = 3$	-2.6221080	1.682538

Outcomes and talks

The numerical results for momentum using energy equations were examined in this study. It is possible to view and discuss in detail the effects of pertinent limitations on the velocity and temperature profile. The important comments that followed were obtained.

- Fluid velocity and temperature increase with increase in Prandtl number Pr , mixed convection restriction λ , Suction restriction S , and exponential Restriction N , while reverse effect is seen in magnetic restriction M , radiation restriction Ra , thermal slip restriction S_t , and heat Source restriction δ ,
- Fluid velocity increases with increase in permeability restriction K , and velocity slip restriction S_v , while reverse effect is seen in Eckert number Ec .
- Skin friction coefficient and Nusselt number both are increasing function of radiation restriction Ra , while reverse effect is seen in magnetic restriction M , and exponential Restriction N .
- Skin friction coefficient is increasing function and Nusselt number is decreasing function of restriction velocity slip restriction S_v while reverse effect is seen in radiation restriction Ra , and heat Source restriction δ .
- Skin friction coefficient is increasing function of Prandtl number Pr and mixed convection restriction λ while reverse effect is seen Suction restriction S , and thermal slip restriction S_t .

References

1. M. I. Char, Heat transfer of a continuous, stretching surface with suction or blowing. *J. Math. Anal. Appl.* 135(2), 568-580 (1988)
2. V. Kumaran, G. Ramanaiah, A note on the flow over a stretching sheet. *Acta Mech.* 116(1), 229-233 (1996)
3. E. Magyari, B. Keller, Heat and mass transfer in the boundary layers on an exponentially stretching continuous surface. *J. Phys. D: Appl. Phys.* 32(5), 577(1999)
4. E. M. A. Elbashbeshy, Heat transfer over an exponentially stretching continuous surface with suction. *Arch. Mech.* 53(6), 643-651 (2001)
5. H. I. Andersson, Slip flow past a stretching surface. *Acta Mech.* 158(1), 121-125 (2002)
6. M. Miklavcic, C. Wang, Viscous flow due to a shrinking sheet. *Q. Appl. Math.* 64(2), 283-290 (2006)
7. F. Aman, A. Ishak, Hydromagnetic flow and heat transfer adjacent to a stretching vertical sheet with prescribed surface heat flux. *Heat Mass Transf.* 46, 615-620 (2010)
8. D. Pal, P. S. Hiremath, Computational modelling of heat transfer over an unsteady stretching surface embedded in a porous medium. *Meccanica.* 45, 415-424 (2010)
9. M. Z. Salleh, R. Nazar, I. Pop, Boundary layer flow and heat transfer over a stretching sheet with Newtonian heating. *J. Taiwan Inst. Chem. Eng.* 41(6), 651-655 (2010)
10. A. Ishak, MHD boundary layer flow due to an exponentially stretching sheet with radiation effect. *Sains Malays.* 40(4), 391-395 (2011)
11. S. Yao, T. Fang, Y. Zhong, Heat transfer of a generalized stretching/shrinking wall problem with convective boundary conditions. *Commun. Nonlinear Sci. Numer. Simul.* 16(2), 752-760 (2011)
12. R. Cortell, Heat transfer in a fluid through a porous medium over a permeable stretching surface with thermal radiation and variable thermal conductivity. *Can. J. Chem. Eng.* 90(5), 1347-1355 (2012).
13. T. Hayat, M. Awais, S. Obaidat, Three-dimensional flow of a Jeffery fluid over a linearly stretching sheet. *Commun. Nonlinear Sci. Numer. Simul.* 17(2), 699-707 (2012).
14. S. K. Soid, S. A. Kechil, A. H. M. Shah, N. Z. Ismail, S. N. S. A. Halim, Hydromagnetic boundary layer flow over stretching surface with thermal radiation. *World Appl. Sci. J.* 17, 33-38 (2012)
15. I. C. Mandal, S. Mukhopadhyay, Heat transfer analysis for fluid flow over an exponentially stretching porous sheet with surface heat flux in porous medium. *Ain Shams Eng. J.* 4(1), 103-110 (2013)
16. S. Mukhopadhyay, slip effects on MHD boundary layer flow over an exponentially stretching sheet with suction/blowing and thermal radiation. *Ain Shams Eng. J.* 4(3), 485-491 (2013)
17. N. M. Sarif, M. Z. Salleh, R. Nazar, Numerical solution of flow and heat transfer over a stretching sheet with Newtonian heating using the Keller box method. *Procedia Eng.* 53, 542-554 (2013).
18. G. Singh, O. D. Makinde, Mixed convection slip flow with temperature jump along a moving plate in presence of free stream. *Therm. Sci.* 19(1), 119-128 (2015)